

Surface Morphology and Conductivity of Ag-Coated Cu Flakes Prepared by Electroless Ag Plating Using Different Additives

Ji Hwan Kim and Jong-Hyun Lee*

Department of Materials Science and Engineering, Seoul National University of Science and Technology, Seoul 01811, Republic of Korea

Ag-coated Cu flakes, several micrometres in size, were fabricated by electroless Ag plating using various complexing and reducing agents to prevent oxidation of Cu flakes, used as a filler material in conductive pastes, during curing in air at <200 °C. The surface morphology and the roughness of the samples depended on the complexing and the reducing agents used. X-ray photoelectron spectroscopy analysis indicated that surface oxidation of Cu by ammonium hydroxide occurs during the Ag plating process, resulting in the formation of needle-shaped particles comprising copper oxide on the surface of Ag-coated Cu flakes. The electrical resistivities of isotropic conductive pastes containing Ag-coated Cu flakes prepared using ammonium hydroxide/potassium L-tartrate, ammonium hydroxide/succinimide, and ethylene diamine tetraacetic acid were 2.8×10^{-3} , 2.5×10^{-3} , and $6.1 \times 10^{-4} \Omega \cdot \text{cm}$, respectively. Ammonium hydroxide oxidizes the flakes during Ag plating to form slight oxide phases on its surface, thereby decreasing the electrical conductivity of the conductive paste.

Keywords: Ag-Coated Cu, Electroless Silver Plating, Complexing Agent, Reducing Agent, Electrical Resistivity.

1. INTRODUCTION

Isotropic conductive pastes (ICPs) have become an indispensable assembly material in microelectronics manufacturing as using them involves simple processing methods and low processing temperatures.^{1–6} In addition, the use of ICPs is expected to increase further with the continuous expansion of reel-to-reel manufacturing of next-generation flexible electronics.^{7–11} Typical ICPs are composed of resin matrices (resin formulations) and electrically conductive fillers. Ag flake is conventionally used as a filler material owing to its excellent electrical, contact, and anti-oxidation properties.^{12–16} However, the high material cost of Ag is one of the main factors that limit the wide use of ICPs in microelectronics.

Ag-coated Cu fillers have been considered as one of the most promising low-cost electrically conductive fillers, and they have been widely investigated since Cu has an electrical conductivity similar to that of Ag.^{17,18} Cu acts as a low-cost core material and the Ag coating functions as an anti-oxidation layer and the contact surface. The Ag

coating layers are conventionally fabricated by electroless plating.^{19,20}

The use of Ag-coated Cu fillers at curing temperatures below 200 °C and studies to achieve a low electrical resistivity have been reported in the literature.^{16,19,21–23} Zhang et al. succeeded in reducing the electrical resistivity of a cured ICP strip from 1.3×10^{-3} to $2.4 \times 10^{-4} \Omega \cdot \text{cm}$ by using Ag-coated Cu flakes surface-treated with an amine-based silane coupling agent.²³ Nishikawa et al. also reported an electrical resistivity of approximately $1.5 \times 10^{-4} \Omega \cdot \text{cm}$ by using Ag-coated Cu spheres with a diameter of 5 μm and presented the effects of the shape and the surface morphology of filler particles on the electrical resistivity.¹⁶ Although the surface modification by chemical treatments and filler particle shape are crucial factors affecting the electrical resistivity of ICP containing Ag-coated Cu fillers, the Ag electroless plating method is also expected to influence the resistivity eventually as it determines the quality of the Ag shell. Therefore, in this study, the properties of Ag shells were characterized after the preparation of Ag-coated Cu flakes using three different combinations of complexing and reducing agents. Furthermore, the effect of surface properties of the Ag-coated

*Author to whom correspondence should be addressed.

Cu flakes on the electrical conductivity of cured films containing the Ag-coated Cu flakes were studied, and the results indicated that Ag-coated Cu filler material exhibits excellent electrical properties.

2. EXPERIMENTAL DETAILS

To remove the surface oxide layer on the as-received Cu flake, a solution was prepared by dissolving 0.15 M ammonium hydroxide (NH_4OH , 28.0–30.0% NH_3 basis, Sigma-Aldrich) and 0.0375 M ammonium sulphate ($(\text{NH}_4)_2\text{SO}_4$, >99%, Sigma) in 100 mL distilled water. Then, 3 g of Cu flakes (D_{50} : 4.9 μm , Duksan Hi-Metal Co., Ltd.) was added to this solution, and the mixture was stirred for 2 min using a magnetic bar. After sedimentation of the Cu flakes, the supernatant was discarded, and the remnant Cu flakes were washed with distilled water four times.

Plating solutions were prepared using different methods. In one method, the 3 g of Cu flakes obtained according to the above-mentioned procedure was added to 95 mL of aqueous solution containing 5 mL ammonium hydroxide/0.2 M potassium L-tartrate ($\text{C}_4\text{H}_5\text{KO}_6$, 99%, Sigma-Aldrich). Henceforth, this solution is referred to as the plating solution. An Ag precursor solution was prepared by dissolving 50 mM of silver nitrate (AgNO_3 , >99.8% Daejung Chemicals and Metals Co., Ltd.) in 5 mL ammonium hydroxide. The amount of AgNO_3 was selected to obtain Ag-coated Cu flakes with 15 wt% Ag. Finally, the Ag precursor solution was added to the plating solution containing Cu flakes under constant stirring. The mixture was stirred for 20 min. The Ag-coated Cu flakes obtained were rinsed using distilled water and ethanol and dried in a low-vacuum chamber for 10 h.

In another method, the 3 g of Cu flakes obtained was added to 100 mL of distilled water. Ag precursor solutions were prepared either by dissolving 50 mM of silver nitrate and 16.9 M succinimide ($\text{C}_4\text{H}_5\text{NO}_2$, 100%, Sigma-Aldrich) in 5 mL ammonium hydroxide or by dissolving 50 mM of silver nitrate, 0.6 M ethylene diamine tetraacetic acid (EDTA, $\text{C}_{10}\text{H}_{16}\text{N}_2\text{O}_8$, 98.5%, Daejung Chemicals & Metals Co., Ltd.), and 2.5 M NaOH (99%, Sooshin Chemical) in 100 mL distilled water. The Ag precursor solutions were added to the solution containing Cu flakes under constant stirring. The mixtures prepared using ammonium hydroxide/succinimide and EDTA were stirred for 60 and 10 min, respectively. Ammonium hydroxide was used for dissolving potassium L-tartrate or succinimide in distilled water, as it was insoluble otherwise.

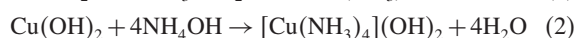
The surface morphology of the dried Ag-coated Cu flakes was examined using scanning electron microscopy (SEM, JSM-7500F, JEOL Ltd.; VEGA3, Tescan). To examine the chemisorbed species and the oxidation state of the surface of Ag-coated Cu flakes, Fourier-transform infrared spectroscopy (FT-IR) and X-ray photoelectron spectroscopy (XPS) were employed. The resistivity of the ICPs was calculated from the

bulk resistance of the film pattern of specific dimensions. The ICP was prepared using a mixture of epoxy (bisphenol-A type liquid epoxy resin diluted with aliphatic glycidyl ether, YD-114; epoxide equivalent weight: 190–210; Kukdo Chemical Co., Ltd.), curing agent (imidazole, CUREZOL 2E4MZ, Shikoku Chemicals Co.), and 69.8 wt% of Ag-coated Cu flakes. It was printed on a glass slide through a stencil mask with a slit volume of $10 \times 10 \times 1 \text{ mm}^3$ using a squeegee. The ICP pattern filled with the Ag-coated Cu flakes was completed by curing the mixture in air at 150 °C for 2 h. The resistance (R) of the cured ICP pattern was measured with a four-point probe linked to a source meter (2400, Keithley). The total distance between the probes set at an interval of 1 mm was 3 mm. The resistivity ρ was calculated from the equation $\rho = (Rtw)/l$, where t , w , and l are the thickness, width, and length of the pattern, respectively.

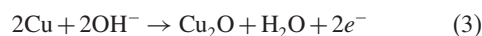
3. RESULTS AND DISCUSSION

Figure 1 shows the SEM images of the Ag-coated Cu flakes prepared using different plating solutions. The Ag-coated Cu flakes prepared with the plating solution containing ammonium hydroxide/potassium L-tartrate exhibit several holes on the surface with some of the flakes losing the initial shape (Fig. 1(a)). The sample prepared with the solution containing ammonium hydroxide/succinimide (Fig. 1(b)) exhibits relatively lesser number of holes and lower surface roughness as compared to the sample prepared with the solution containing ammonium hydroxide/potassium L-tartrate. Ag-coated Cu flakes with a smooth surface were obtained using the solution containing EDTA (Fig. 1(c)). These results indicate that the additives in the plating solution affect the surface morphology of the Ag-coated Cu flakes.

The changes in the number of holes on the Ag-coated Cu flake surfaces as seen in Figure 1 can be attributed to the addition of ammonium hydroxide in the plating solution. Ammonium hydroxide is commonly used to remove oxide or hydroxide (Cu_2O , $\text{Cu}(\text{OH})_2$) layer on the surface of Cu flakes using the following reactions:^{24–26}



As per reactions (1) and (2), the thin oxide or hydroxide layer present on the Cu flakes is completely removed on pretreatment with ammonium hydroxide, resulting in pure Cu surfaces. However, ammonium hydroxide also takes part in a side reaction, forming oxides or hydroxides on pure Cu surface. When the pure Cu surface is exposed to ammonium hydroxide, Cu_2O or $\text{Cu}(\text{OH})_2$ phase can be formed on the surface according to the following reactions.^{27–29}



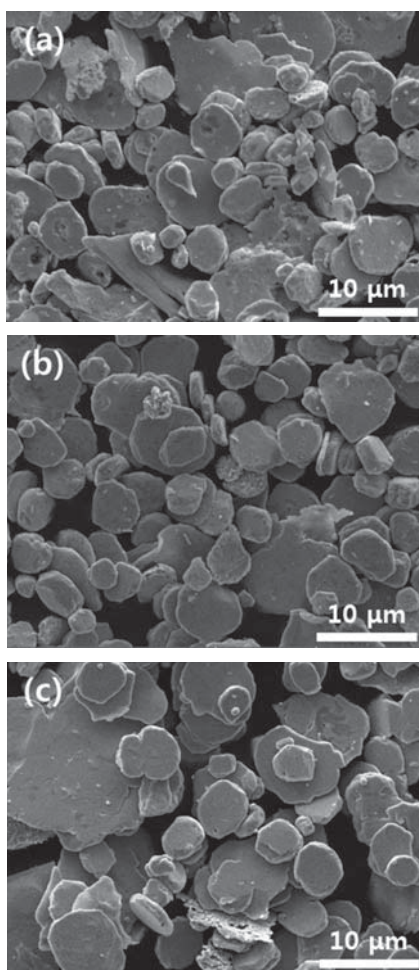


Fig. 1. Low-magnification SEM images of the Ag-coated Cu flakes prepared using different additives during the plating process: (a) Ammonium hydroxide/potassium L-tartrate, (b) ammonium hydroxide/succinimide, and (c) EDTA.

These oxides or hydroxides would inhibit the galvanic displacement reaction between Cu atom and the Ag complex ion ($\text{Ag}(\text{NH}_3)_2^+$) formed with Ag and ammonium ions and accelerate the formation of individual or nodule-shaped Ag nanoparticles instead of Ag plating layers during the reduction of the Ag complex ion. Hence, smooth Ag coating layers on the Cu flake surfaces cannot be achieved. Ammonium hydroxide in the plating solution can remove the formed oxide and hydroxide again; therefore, reformation and removal of Cu_2O and $\text{Cu}(\text{OH})_2$ on the surface of the Cu flakes would occur repeatedly until all the ammonium hydroxide is eliminated. This process results in the formation of holes.³⁰ Thus, the plating solution containing ammonium hydroxide causes the formation of holes on the Cu flakes during plating, and the number of holes increases with an increase in the ammonium hydroxide concentration and the plating time.

Figure 2 shows the high-magnification SEM images of the Ag-coated Cu flakes prepared using different plating solutions. Many tiny needle-shaped particles are observed on the surface of the Ag-coated Cu flakes prepared with the Ag plating solution containing ammonium hydroxide/potassium L-tartrate (Fig. 2(a)), indicating the formation of relatively rough surfaces. In the case of the samples prepared using the plating solution containing ammonium hydroxide/succinimide (Fig. 2(b)), less number of needle-shaped particles and decreased surface roughness are observed as compared to the sample prepared with the solution containing ammonium hydroxide/potassium L-tartrate. Needle-shaped particles are not observed on the surface of the Ag-coated Cu flakes obtained using the solution containing EDTA (Fig. 2(c)), resulting in the formation of a compact and smooth Ag coating layer. Overall, the number of needle-shaped particles increases with an increase in the ammonium hydroxide concentration.

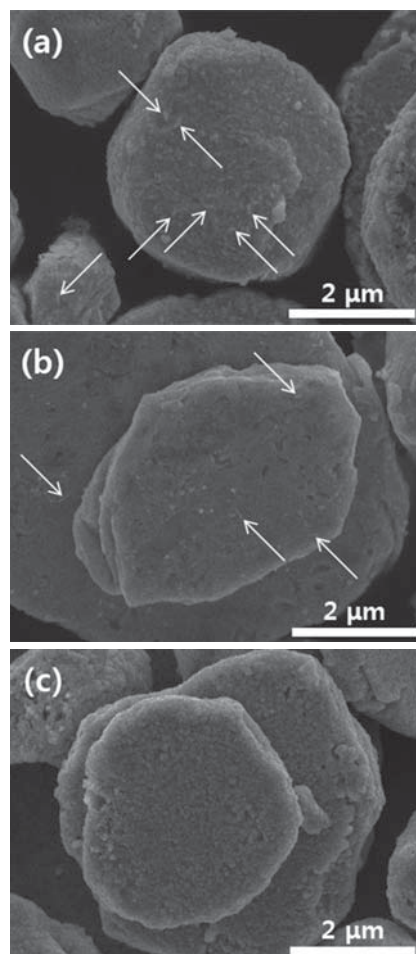


Fig. 2. High-magnification SEM images of the Ag-coated Cu flakes prepared using different additives during the plating process: (a) Ammonium hydroxide/potassium L-tartrate, (b) ammonium hydroxide succinimide, and (c) EDTA.

The FT-IR spectra of the Ag-coated Cu flakes prepared using different plating solutions were recorded for examining the chemisorbed species on the surface of the Ag-coated Cu flakes and identifying the composition of the needle-shaped particles; the results are shown in Figure 3. Peaks are observed in the range of 3421–3438 cm^{-1} for all the samples, which could be attributed to OH stretching vibrations due to moisture absorbed on the surface of Ag-coated Cu flakes.^{31–33} A peak is observed at 1628 cm^{-1} , which corresponds to OH bending mode arising from moisture on the surface.^{31–33} In the fingerprint region, different minor peaks of additives are observed for different samples. However, the intensities of the peaks are very low to identify the additives adsorbed on the surface. The peaks observed at 2860 and 2930 cm^{-1} for all the samples correspond to symmetrical and asymmetrical CH_2 stretching vibrations, respectively, implying the presence of traces of additives on the surface.^{34–36} The intensities of these peaks are also very low to confirm absorption by additives. Thus, the tiny needle-shaped particles on the Ag-coated Cu flakes could not be characterized by the FT-IR measurements.

To obtain more information about the surface composition of the Ag-coated Cu flakes, XPS measurements were performed. The Cu $2p_{3/2}$ XPS spectrum is shown in Figure 4. Regardless of the type of additives used, all the samples exhibit peaks at 932.6, 932.8, and 934.6 eV, corresponding to the zero-valent Cu, $\text{Cu}^+(\text{Cu}_2\text{O})$, and $\text{Cu}^{2+}(\text{CuO})$, respectively.^{37–44} The broad peaks at 942.34 and 944.52 eV correspond to the Cu^{2+} satellite peak.^{45–47} These satellite peaks result from charge transfer transitions from ligands (O^{2-} ions for CuO) into the unfilled (d^9) valence level of a Cu^{2+} ion.^{46,48} For Cu^+ ion with a filled (d^{10}) ground state configuration, such transitions cannot occur and satellite peaks are not observed.

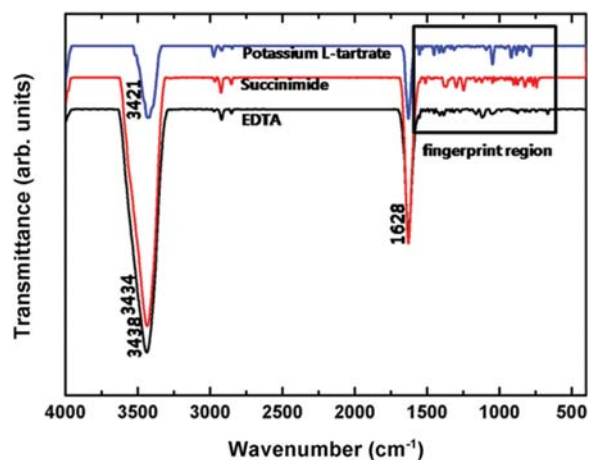


Fig. 3. FT-IR spectra of the Ag-coated Cu flakes prepared using different plating solutions.

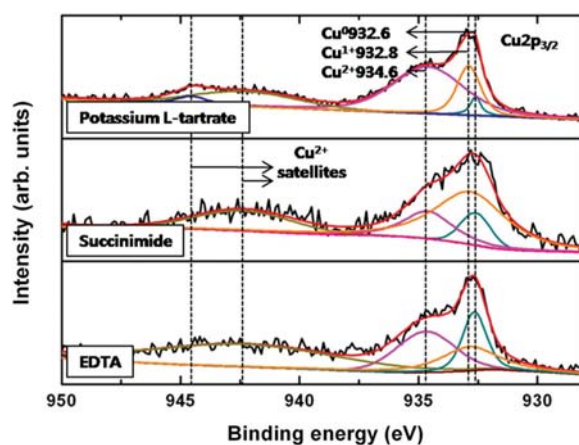


Fig. 4. XPS spectra of the Ag-coated Cu flakes prepared using different plating solutions.

To investigate the surface oxidation state, the integrated intensity of each peak and related information were examined, and the results are presented in Table I. We calculated the ratio of pure Cu to Cu oxide (integrated intensity of zero-valent Cu peak/integrated intensity of Cu oxide peak, $I_{\text{Cu}^0}/I_{\text{Cu oxide}}$) using the equation:

$$\frac{I_{\text{Cu}}}{I_{\text{Cu oxide}}} = \frac{I_{\text{Cu}^0}}{I_{\text{Cu}^{2+}} + I_{\text{Cu}^+}} \quad (5)$$

where I_{Cu^0} , $I_{\text{Cu}^{2+}}$, and I_{Cu^+} represent the integrated intensities of zero-valent Cu, Cu^{2+} , and Cu^+ , respectively. The $I_{\text{Cu}^0}/I_{\text{Cu oxide}}$ ratios for samples prepared with potassium L-tartrate, succinimide, and EDTA, were 0.05, 0.14, and 0.38, respectively. This indicates that surface oxidation by ammonium hydroxide occurs during the Ag plating process with the addition of potassium L-tartrate or succinimide. Moreover, the degree of surface oxidation increases with an increase in the ammonium hydroxide concentration. Therefore, the needle-shaped particles observed on the surface of Ag-coated Cu in the SEM images in Figures 2(a) and (b) are expected to consist of Cu oxide phases. When EDTA was used, ammonium hydroxide was not included in the Ag plating solution; in this case, the oxidation of Cu would decelerate and the amount of non-oxidized Cu would increase, as shown in Figure 4 and Table I.

Figure 5 shows the electrical resistivities of the cured films of the ICPs filled with the Ag-coated Cu flakes prepared using different plating solutions. The bulk resistivities of the ICPs filled with the Ag-coated Cu flakes

Table I. Integrated intensities of XPS peaks of the Ag-coated Cu flakes prepared using different additives and related information.

Additive	$I_{\text{Cu}^{2+}}$	$I_{\text{Cu}^{1+}}$	I_{Cu^0}	$I_{\text{Cu}^0}/(I_{\text{Cu}^{2+}} + I_{\text{Cu}^{1+}})$
Potassium L-tartrate	5427	1949	388	0.05
Succinimide	902	2545	503	0.14
EDTA	1989	1488	1353	0.38

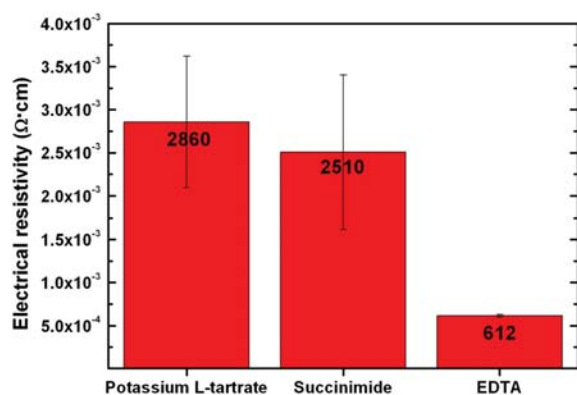


Fig. 5. Electrical resistivities of the cured films of ICPs filled with the Ag coated Cu flakes prepared using different plating solutions.

prepared using potassium L-tartrate, succinimide, and EDTA are approximately 2.8×10^{-3} , 2.5×10^{-3} , and $6.1 \times 10^{-4} \Omega \cdot \text{cm}$, respectively. Hence, the electrical conductivity of pastes containing metal particles depends on the surface oxidation state of the conductive particles as well as the surface defects on the conductive particles, such as holes. If oxides with no or low electrical conductivity are present on the surface of the conductive particles, the electrical conductivity of the conductive paste reduces, because electrical conduction is accomplished by contact between the conductive particles. The presence of ammonium hydroxide in the plating solution leads to the formation of defects and huge Cu oxide particles on the surface of Ag-coated Cu flakes during Ag plating. Hence, the electrical resistivities of the ICPs filled with the Ag-coated Cu flakes prepared using potassium L-tartrate and succinimide are relatively high. Further, defect formation and Cu oxidation on the surface of flakes are suppressed when EDTA is added to the plating solution. Therefore, the electrical resistivity of the ICP containing Ag-coated Cu flakes fabricated using EDTA is relatively low.

4. CONCLUSION

The surface morphology and the roughness of Ag-coated Cu flakes after Ag plating were found to depend strongly on the type of complexing and reducing agents used. X-ray photoelectron spectroscopic analysis of the Ag-coated Cu flakes indicated that surface oxidation of Cu occurs with the addition of ammonium hydroxide during the Ag plating process. In addition, the oxidation degree increased with an increase in the ammonium hydroxide concentration, and the needle-shaped particles observed on the surface of the Ag-coated Cu flakes consisted of Cu oxide phases. The electrical resistivities of the cured films of isotropically conductive paste containing Ag-coated Cu flakes prepared using ammonium hydroxide/potassium L-tartrate, ammonium hydroxide/succinimide, and EDTA were 2.8×10^{-3} , 2.5×10^{-3} , and $6.1 \times 10^{-4} \Omega \cdot \text{cm}$,

respectively. The paste containing Ag-coated Cu flakes prepared using EDTA, in the absence of ammonium hydroxide, exhibited the lowest resistance value as the formation of Cu oxide was suppressed.

Acknowledgments: This work was supported by Nano-Convergence Foundation (www.nanotech2020.org) funded by the Ministry of Science, ICT and Future Planning (MSIP, Korea) and the Ministry of Trade, Industry and Energy (MOTIE, Korea; Project Name: Commercialization of 100 Gbps optical receiver and transmitter modules based on nano Ag-coated Cu paste; Project Number: R201503310). The authors also thank Korean Basic Science Institute (KBSI) for FT-IR and XPS analyses.

References and Notes

1. K. J. C. Jagt, *IEEE Trans. Compon. Packag. Manuf. Technol. A* 21, 215 (1998).
2. D. Wojciechowski, J. Vanfleteren, E. Reese, and H.-W. Hagedorn, *Microelectron. Reliab.* 40, 1215 (2000).
3. M. Inoue and K. Suganuma, *J. Electron. Mater.* 36, 669 (2007).
4. M. Inoue, H. Muta, T. Maekawa, S. Yamanaka, and K. Suganuma, *J. Electron. Mater.* 37, 462 (2008).
5. D.-H. Kim, S. Yoo, C.-W. Lee, and T.-Y. Lee, *J. Microelectron. Packag. Soc.* 17, 55 (2010).
6. Y.-S. Eom, K.-S. Choi, S.-H. Moon, J.-H. Park, J.-H. Lee, and J.-T. Moon, *ETRI J.* 33, 864 (2011).
7. I. Mir and D. Kumar, *Int. J. Adhes. Adhes.* 28, 362 (2008).
8. J. C. Jagt, P. J. M. Beris, and G. F. C. M. Lijten, *IEEE Trans. Compon. Packag. Manuf. Technol. B* 18, 292 (1995).
9. D. Huang, F. Liao, S. Moles, D. Redinger, and V. Subramanian, *J. Electrochem. Soc.* 150, G412 (2003).
10. A. C. Siegel, S. T. Phillips, M. D. Dickey, N. Lu, Z. Suo, and G. M. Whitesides, *Adv. Funct. Mater.* 20, 28 (2010).
11. M. Schrödner, S. Sensfuss, H. Schache, K. Schultheis, T. Welzel, K. Heinemann, R. Milker, J. Marten, and L. Blankenburg, *Sol. Energy Mater. Sol. Cells* 107, 283 (2012).
12. Y. Li, K.-S. Moon, and C. P. Wong, *J. Appl. Polym. Sci.* 99, 1665 (2006).
13. X. Luo, G. A. Gelves, U. Sundararaj, and J.-L. Luo, *Can. J. Chem. Eng.* 91, 630 (2013).
14. H. T. Hai, J. G. Ahn, D. J. Kim, J. R. Lee, H. S. Chung, and C. O. Kim, *Surf. Coat. Technol.* 201, 3788 (2006).
15. B. K. Park, D. Kim, S. Jeong, J. Moon, and J. S. Kim, *Thin Solid Films* 515, 7706 (2007).
16. H. Nishikawa, S. Mikami, K. Miyake, A. Aoki, and T. Takemoto, *Mater. Trans.* 51, 1785 (2010).
17. G. A. Gelves, B. Lin, U. Sundararaj, and J. A. Haber, *Adv. Funct. Mater.* 16, 2423 (2006).
18. R. Manepalli, F. Stepniak, S. A. Bidstrup-Allen, and P. A. Kohl, *IEEE Trans. Adv. Packag.* 22, 4 (1999).
19. G. Kim, K.-M. Jung, J.-T. Moon, and J.-H. Lee, *J. Microelectron. Packag. Soc.* 21, 51 (2014).
20. J. Zhao, D. Zhang, and J. Zhao, *J. Solid State Chem.* 184, 2339 (2011).
21. M. Grouchko, A. Kamysny, and S. Magdassi, *J. Mater. Chem.* 19, 3057 (2009).
22. R. Zhang, W. Lin, K. S. Moon, Q. Liang, and C. P. Wong, *IEEE Trans. Compon. Packag. Manuf. Technol.* 1, 25 (2011).
23. R. Zhang, W. Lin, K. Lawrence, and C. P. Wong, *Int. J. Adhes. Adhes.* 30, 403 (2010).
24. J. Xu, W. Zhang, Z. Yang, and S. Yang, *Inorg. Chem.* 47, 699 (2008).
25. Q. Luo, R. A. Mackay, and S. V. Babu, *Chem. Mater.* 9, 2101 (1997).

26. P. Shi, Q. Wang, Y. Xu, and W. Luo, *Mater. Lett.* 65, 857 (2011).
27. D. W. Shoesmith, S. Sunder, M. G. Bailey, G. J. Wallace, and F. W. Stanchell, *J. Electroanal. Chem. Interfacial Electrochem.* 143, 153 (1983).
28. C. Lu, L. Qi, J. Yang, D. Zhang, N. Wu, and J. Ma, *J. Phys. Chem. B* 108, 17825 (2004).
29. X. Wen, W. Zhang, and S. Yang, *Langmuir* 19, 5898 (2003).
30. J. H. Kim and J.-H. Lee, *Korean J. Mater. Res.* 24, 617 (2014).
31. S.-Y. Lin, S.-L. Wang, Y.-S. Wei, and M.-J. Li, *Surf. Sci.* 601, 781 (2007).
32. H. A. Al-Abadleh and V. H. Grassian, *Langmuir* 19, 341 (2003).
33. L. M. Proniewicz, C. Paluszkiwicz, A. Wesełucha-Birczyńska, H. Majcherczyk, A. Barański, and A. Konieczna, *J. Mol. Struct.* 596, 163 (2001).
34. A. Sárkány, A. H. Weiss, T. Szilágyi, P. Sándor, and L. Guzzi, *Appl. Catal.* 12, 373 (1984).
35. J. Schmitt and H.-C. Flemming, *Int. Biodeterior. Biodegrad.* 41, 1 (1998).
36. C. Chang, B. Duan, J. Cai, and L. Zhang, *Eur. Polym. J.* 46, 92 (2010).
37. R. J. Bird and P. Swift, *J. Electron Spectrosc. Relat. Phenom.* 21, 227 (1980).
38. J. Batista, A. Pintar, D. Mandrino, M. Jenko, and V. Martin, *Appl. Catal. Gen.* 206, 113 (2001).
39. M. Finšgar, *Corros. Sci.* 77, 350 (2013).
40. M. Yin, C.-K. Wu, Y. Lou, C. Burda, J. T. Koberstein, Y. Zhu, and S. O'Brien, *J. Am. Chem. Soc.* 127, 9506 (2005).
41. M. P. Seah, G. C. Smith, and M. T. Anthony, *Surf. Interface Anal.* 15, 293 (1990).
42. I. Grohmann, B. Peplinski, and W. Unger, *Surf. Interface Anal.* 19, 591 (1992).
43. V. D. Castro, C. Furlani, M. Gargano, and M. Rossi, *Appl. Surf. Sci.* 28, 270 (1987).
44. S. Carniato, H. Roulet, G. Dufour, S. Palacin, A. Barraud, P. Millie, and I. Nenner, *J. Phys. Chem.* 96, 7072 (1992).
45. Z. Mekhalif, F. Sinapi, F. Laffineur, and J. Delhalle, *J. Electron Spectrosc. Relat. Phenom.* 121, 149 (2001).
46. C. C. Chusuei, M. A. Brookshier, and D. W. Goodman, *Langmuir* 15, 2806 (1999).
47. S. Poulston, P. M. Parlett, P. Stone, and M. Bowker, *Surf. Interface Anal.* 24, 811 (1996).
48. K. S. Kim, *J. Electron Spectrosc. Relat. Phenom.* 3, 217 (1974).

Received: 26 October 2017. Accepted: 9 July 2018.